IRIS RECOGNITION SYSTEM

MAJOR PROJECT SUBMITTED IN PARTIAL FULFILLMENT OF THE REQUIREMENTS FOR THE AWARD OF DEGREE OF

Master of Technology

In

Information Systems

Submitted By:

AKSHAT JAIN

(2K12/ISY/01)

Under the Guidance of

Prof. O. P. Verma

(HOD, Department of IT)

DEPARTMENT OF INFORMATION TECHNOLOGY

DELHI TECHNOLOGICAL UNIVERSITY

(2012-2014)

ABSTRACT

Iris Recognition is one of the most important biometric recognition systems to authenticate people. Iris recognition works by matching the iris patterns of two individuals. In this paper an efficient iris recognition system is proposed. The process used herein concentrates on image segmentation, normalization, feature extraction and encoding, and verification. Segmentation is done with the help of a great mix of Integro-Differential operator and Hough transformation. This approach provides you with better noise reduction and better iris deduction. Normalization of iris region is performed using the rubber sheet model of Daugman. Next, the properties of Gabor Filters are used to extract the features from the iris. Finally, matching of two templates or two iris-codes is performed by using the hamming distance formula to decide among imposters and genuine ones. The principle of operation used behind iris recognition system is the failure of a test of statistical independence and distinctiveness of the iris texture. This system gives better results than Libor Masek's system, in terms of efficiency and in terms of time complexity. The proposed system gives better results than Libor Masek's system, in terms of efficiency and time complexity. The proposed system performed more than 52900 comparisons for authentication on a set of 230 eye images. These images were taken from CASIA-IrisV4-Sync database.

ACKNOWLEDGEMENT

I take the opportunity to express my sincere gratitude to my project mentor Dr. O.P. Verma, Head of Department, Department of Information Technology, Delhi Technological University, Delhi for providing valuable guidance and constant encouragement throughout the project. It is my pleasure to record my sincere thanks to him for his constructive criticism and insight without which the project would not have shaped as it has.

I humbly extend my words of gratitude to other faculty members of this department for providing their valuable help and time whenever it was required.

Akshat Jain
Roll No. 2K12/ISY/01
M.Tech (Information Systems)
E-mail: akshat.dtu@gmail.com

CERTIFICATE

This is to certify that the thesis entitled, **"Iris Recognition System"** submitted by **Akshat Jain (2K12/ISY/01)** in partial fulfillment of the requirements for the award of Master of Technology Degree in Information Systems during session 2012-2014 at Delhi Technological University is an authentic work carried out by him under my supervision and guidance.

To the best of my knowledge, the matter embodied in the thesis has not been submitted to any other University / Institute for the award of any Degree or Diploma.

Dr. O. P. Verma
Head of Department
Department of Information Technology
Delhi Technological University
Delhi

TABLE OF CONTENTS

LIST OF FIGURES

LIST OF TABLES

CHAPTER 1
INTRODUCTION

1.1 BIOMETRIC TECHNOLOGY

A biometric system provides automatic recognition of an individual based on some sort of unique feature or characteristic possessed by the individual. Biometric systems have been developed based on fingerprints, facial features, voice, hand geometry, handwriting, the retina, and the one presented in this thesis, the iris.

Biometric systems work by first capturing a sample of the feature, such as recording a digital sound signal for voice recognition, or taking a digital color image for face recognition. The sample is then transformed using some sort of mathematical function into a biometric template. The biometric template will provide a normalized, efficient and highly discriminating representation of the feature, which can then be objectively compared with other templates in order to determine identity. Most biometric systems allow two modes of operation. An enrolment mode for adding templates to a database, and an identification mode, where a template is created for an individual and then a match is searched for in the database of pre-enrolled templates.

A good biometric is characterized by use of a feature that is; highly unique – so that the chance of any two people having the same characteristic will be minimal, stable – so that the feature does not change over time, and be easily captured – in order to provide convenience to the user, and prevent misrepresentation of the feature.

1.2 THE HUMAN IRIS

The Intra-tissue Refractive Index Shaping (IRIS) is made up of elastic connective tissue, i.e. the trabecular meshwork, and during the eighth month of gestation its prenatal morphogenesis is completed. The color of the iris often changes during the first year after birth, but the iris pattern, which will be processed and manipulated, is stable throughout the lifespan. Iris is not influenced by the environment as it is an internal organ and is protected by the cornea along with aqueous

humor. But iris area get extracted or contracted due to the illumination of light on the pupil area. Figure 1-1 gives pictorial view of the human iris.

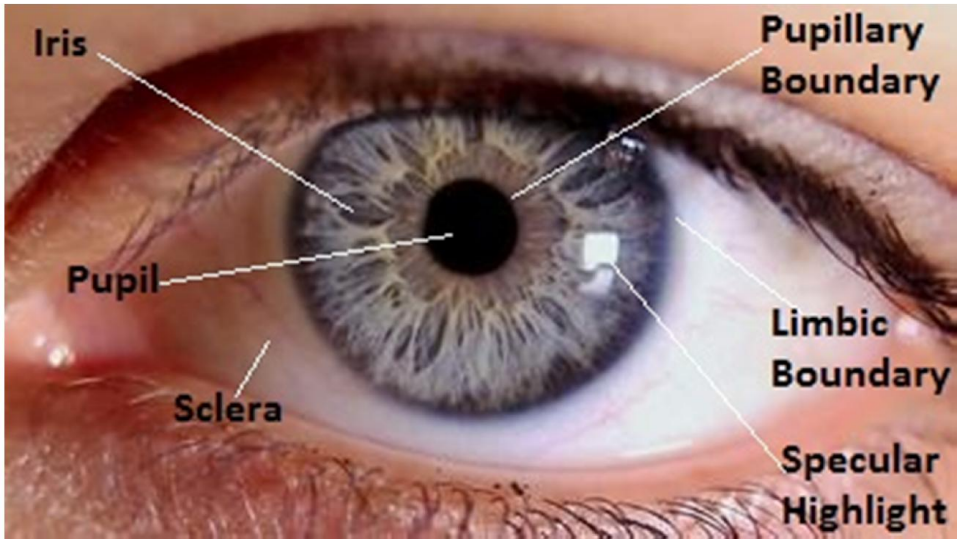

Figure 1-1 A front-on view of the human eye

1.3 A BIOMETRIC SYSTEM

An authentication system based on biometrics is fundamentally a pattern-recognition model which provides an automatic or semi-automatic authentication of a particular person. Recognition is based on a feature or characteristics an individual possesses. It is must that these characteristics are unique. The basic structure of it is as shown in Figure 1-2. Biometric systems can be applied for two purposes: for identification purpose or for verification purpose. Identification means comparison of the acquired biometric information with those templates corresponding to all registered users in the defined database. On the other hand, verification means the comparison of the acquired biometric information against the claimed identity's templates. Hence, identification and verification are two separate problems and these should be considered separately.

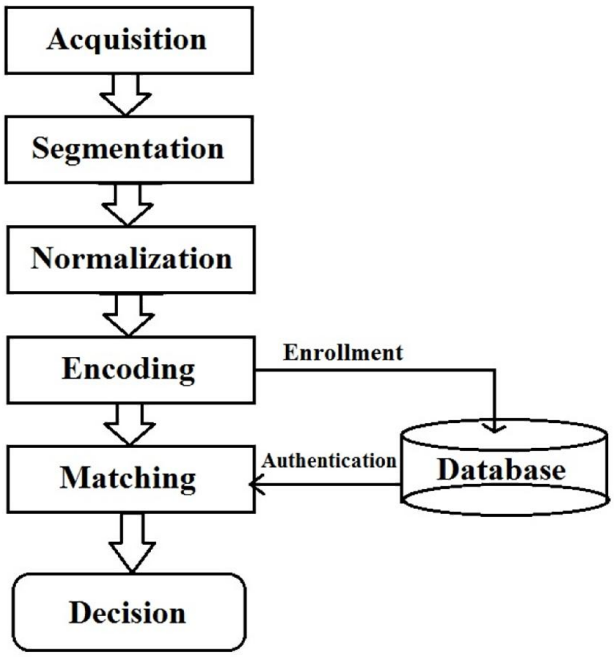

Figure 1-2 A biometric system

1.4 IRIS: A BETTER CANDIDATE FOR BIOMETRICS

The attributes against which a biometric can be evaluated are: 1) the number of degrees-of-freedom, i.e. uniqueness of the characteristics across the human population; 2) its immunity, i.e. it should not be influenced with time and; 3) its patterns should be capable of efficiently encoding and it should be reliable to recognize the individuals by using these patterns. Each individual has a unique iris. The uniqueness of an iris pattern extends to a degree where even the iris patterns of the left and right eye of the same individual do not match. Even identical twins also have different iris structures and hence it is unique. Iris Recognition is considered as the most reliable [7] and the most accurate biometric authentication system available [8].

The need for high security access results in wide usage of the biometric systems. This approach recognizes persons by the result of the statistical independence test based on their iris patterns against enrolled descriptions derived from themselves and everybody else. Specifically, iris Recognition is increasingly used today to enable border-crossing controls, to uniquely identify an individual, to provide access to genuine ones and in many multi-modal biometric systems.

1.5 SCOPE OF IMPROVEMENT

The efficiency or accuracy of IRS extremely depends on two things: proper edge detection or segmentation and accurate template matching. If it is not segmented properly, even a method capable of extracting features accurately would also be unable to obtain useful information from an iris image [13]. Segmentation or extraction of the visible iris portion of the image is a critical step in iris recognition. After extracting this region of interest (ROI) various occluding elements have to be removed such as eyelids, eyelashes and specular highlights. Various region detection and active contour techniques are available to perform these steps.

Also, the result based on simple hamming distance matching is not sufficient to compare two iris templates completely [1]. Sometimes, rotational inconsistencies arise in a template due to difference in illumination settings and the orientation of camera lens, which makes the comparison between templates inaccurate. To handle such inconsistencies, comparisons are made between a pair of templates by rotating one template over the other and such process can be repeated many number of times and compared each time. After this, the best result is chosen from these comparison results. This process removes inconsistencies but increases the time complexity of the system. So, the templates should be rotated only a limited number of times to get reasonable results within reasonable time.

1.6 STATISTICAL DECISION THEORY TO DECIDE AMONG IMPOSTERS AND GENUINE ONES

Two iris codes are compared on the basis of a similarity measure termed as Hamming Distance, which calculates the distance or similarity among the two iris-codes [3], [9]. The number of bits disagreeing in the two codes is computed, and then it is divided by the total number of concerned bits to normalize it (i.e., in the range of [0-1]). So, the Hamming Distance of every iris code with itself would be 0 and similarly, it would be 1 for a comparison between any iris code and its complement. Thus, Hamming Distance of two different iris codes would be 0.5 on an average case and a comparison of two iris codes obtained from same eye at different conditions or occasions, would yield a lower Hamming Distance value but not exactly zero.

A couple of bits A and B with their all combinations are: AB = 00, 01, 10 and 11. The definition of the XOR operator is: If only one of the inputs is 1 then their XOR is 1; otherwise it is 0. Thus,

Table 1-1 shows all combinations of the pair of bits, A and B, with their XOR values. It is clear from this table that to detect a dissimilarity among any pair of bits, XOR operator can be used, whatever their values any disagreement can be detected.

Table 1-1 XOR Operator

A	B	A XOR B
0	0	0
0	1	1
1	0	1
1	1	0

The problem of recognizing an individual is to decide whether he or she is an imposter or an authentic. This problem can be framed within the skeleton of pattern recognition and decision theory as shown in Figure 1-3.

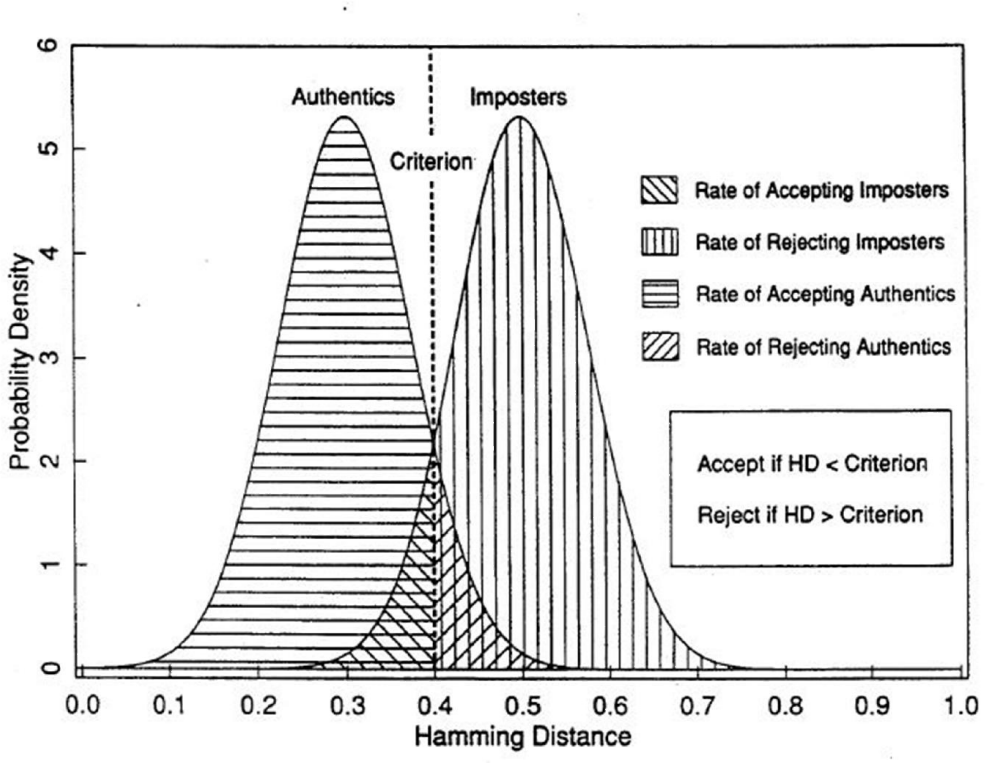

Figure 1-3 Plot showing formulation for statistical decision theory [1]

Four possible outcomes of this pattern recognition are Genuine Acceptance (AG), Imposter Acceptance (AI), Genuine Rejection (RG) and Imposter Rejection (RI). By maximizing the likelihoods of AG and RI and minimizing the likelihoods of AI and RG, genuine and imposter individuals can be located and this is also the goal of the decision-making algorithm. The goal to decide among imposter and authentic is based on the chosen criterion, as indicated by the dashed vertical line in Figure 3. The decision rule is defined as: Accept if Hamming Distance is less than or equal to Criterion and Reject if Hamming Distance is greater than Criterion.

The Authentic distribution, $P_{Au}(H)$ gives the probability of a particular similarity metric H, arising from an authentic. Similarly, imposter distribution, $P_{\text{Imp}}(H)$ gives the probability of a specific similarity metric H, emerging from an imposter. The probabilities of all defined outcomes (AG, AI, RG and RI) are equal to the areas on both side of the selected criterion, C under two ($P_{Au}(H)$ and $P_{\text{Imp}}(H)$) probability functions and are calculated as follows:

$$P(AG) = \int_0^C P_{Au}(H)dH \tag{1}$$

$$P(RG) = \int_C^1 P_{Au}(H)dH \tag{2}$$

$$P(\text{AI}) = \int_0^C P_{\text{Imp}}(H)dH \tag{3}$$

$$P(\text{RI}) = \int_C^1 P_{\text{Imp}}(H)dH \tag{4}$$

Four probabilities (1), (2), (3) and (4) are indicated by the four shaded areas in Figure 1-3. It is direct that to minimize the two error rates, $P(RG)$ and $P(\text{AI})$ or False Rejection Rate (FRR) and False Acceptance Rate (FAR), the overlapped area of the two similarity metric distributions, $P_{\text{Imp}}(H)$ and $P_{Au}(H)$, should be minimized.

1.7 OBJECTIVE

The objective will be to implement an iris recognition system. The development tool used will be MATLAB®, and emphasis will be only on the software for performing recognition, and not hardware for capturing an eye image. A rapid application development (RAD) approach will be

employed in order to produce results quickly. MATLAB® provides an excellent RAD environment, with its image processing toolbox, and high level programming methodology. To test the system, two data sets of eye images will be used as inputs; a database of 230 grey scale eye images courtesy of The Chinese Academy of Sciences– Institute of Automation (CASIA-IrisV4-Sync) [4].

The system is to be composed of a number of sub-systems, which correspond to each stage of iris recognition. These stages are segmentation – locating the iris region in an eye image, normalization – creating a dimensionally consistent representation of the iris region, and feature encoding – creating a template containing only the most discriminating features of the iris. The input to the system will be an eye image, and the output will bean iris template, which will provide a mathematical representation of the iris region.

CHAPTER 2
LITERATURE REVIEW

2.1 SEGMENTATION

The first stage of iris recognition is to isolate the actual iris region in a digital eye image. The iris region, shown in Figure 1-1, can be approximated by two circles, one for the iris/sclera boundary and another, interior to the first, for the iris/pupil boundary. The eyelids and eyelashes normally occlude the upper and lower parts of the iris region. Also, specular reflections can occur within the iris region corrupting the iris pattern. A technique is required to isolate and exclude these artifacts as well as locating the circular iris region. Following is the explanation of various techniques that can be used to segment out the iris region.

2.1.1 Hough Transform

The Hough transform is a standard computer vision algorithm that can be used to determine the parameters of simple geometric objects, such as lines and circles, present in an image. The circular Hough transform can be employed to deduce the radius and center coordinates of the pupil and iris regions. Firstly, an edge map is generated by calculating the first derivatives of intensity values in an eye image and then thresholding the result. From the edge map, votes are cast in Hough space for the parameters of circles passing through each edge point. These parameters are the center coordinates u_c and v_c, and the radius r, which are able to define any circle according to the equation

$$u_c^2 + v_c^2 - r^2 = 0 \tag{5}$$

A maximum point in the Hough space will correspond to the radius and center coordinates of the circle best defined by the edge points. Wildes et al. and Kong and Zhang also make use of the parabolic Hough transform to detect the eyelids, approximating the upper and lower eyelids with parabolic arcs, which are represented as;

$$\left(-\left(u-h_i\right)\sin\theta_i+\left(v-k_i\right)\cos\theta_i\right)^2=a_i\left(\left(u-h_i\right)\cos\theta_i+\left(v-k_i\right)\sin\theta_i\right) \tag{6}$$

Where curvature is controlled by a_i, parabola's peak is $\left(h_i,k_i\right)$ and the rotation angle relative to the x-axis is θ_i.

There are a number of problems with the Hough transform method. First of all, it requires threshold values to be chosen for edge detection, and this may result in critical edge points being removed, resulting in failure to detect circles/arcs. Secondly, the Hough transform is computationally intensive due to its 'brute-force' approach, and thus may not be suitable for real time applications.

2.1.2 Daugman's Integro-differential Operator

Daugman makes use of an integro-differential operator for locating the circular iris and pupil regions, and also the arcs of the upper and lower eyelids. The integro-differential operator is defined as:

$$\max(\mathrm{r},\mathrm{u}_o,\mathrm{v}_o)\left|G_\sigma(r)*\frac{\partial}{\partial r}\oint_{r,\mathrm{u}_o,\mathrm{v}_o}\frac{I(\mathrm{u},\mathrm{v})}{2\pi r}ds\right| \tag{7}$$

Where $I\left(\mathrm{u},\mathrm{v}\right)$ is the eye image, r is the radius to search for, $G_\sigma\left(r\right)$ is a Gaussian smoothing function, and sis the contour of the circle given by r,u_o,v_o. The operator searches for the circular path where there is maximum change in pixel values, by varying the radius and center u and v position of the circular contour. The operator is applied iteratively with the amount of smoothing progressively reduced in order to attain precise localization. Eyelids are localized in a similar manner, with the path of contour integration changed from circular to an arc.

The integro-differential can be seen as a variation of the Hough transform, since it too makes use of first derivatives of the image and performs a search to find geometric parameters. Since it works with raw derivative information, it does not suffer from the thresholding problems of the Hough transform. However, the algorithm can fail where there is noise in the eye image, such as from reflections, since it works only on a local scale.

2.1.3 Active Contour Models

We can make use of active contour models for localizing the pupil in eye images. Active contours respond to pre-set internal and external forces by deforming internally or moving across an image until equilibrium is reached. The contour contains a number of vertices, whose positions are changed by two opposing forces, an internal force, which is dependent on the desired characteristics, and an external force, which is dependent on the image. Each vertex is moved between times t and $t+1$ by

$$v_i(t+1) = v_i(t) + F_i(t) + G_i(t) \tag{8}$$

Where F_i is the internal force, G_i is the external force and v_i is the position of vertex i. For localization of the pupil region, the internal forces are calibrated so that the contour forms a globally expanding discrete circle. The external forces are usually found using the edge information. In order to improve accuracy Ritter et al. use the variance image, rather than the edge image.

A point interior to the pupil is located from a variance image and then a discrete circular active contour (DCAC) is created with this point as its center. The DCAC is then moved under the influence of internal and external forces until it reaches equilibrium, and the pupil is localized.

2.1.4 Eyelash and Noise Detection

Kong and Zhan present a method for eyelash detection, where eyelashes are treated as belonging to two types, separable eyelashes, which are isolated in the image, and multiple eyelashes, which are bunched together and overlap in the eye image. Separable eyelashes are detected using 1D Gabor filters, since the convolution of a separable eyelash with the Gaussian smoothing function results in a low output value. Thus, if a resultant point is smaller than a threshold, it is noted that this point belongs to an eyelash. Multiple eyelashes are detected using the variance of intensity.

If the variance of intensity values in a small window is lower than a threshold, the center of the window is considered as a point in an eyelash. The Kong and Zhang model also makes use of connective criterion, so that each point in an eyelash should connect to another point in an eyelash or to an eyelid. Specular reflections along the eye image are detected using thresholding, since the intensity values at these regions will be higher than at any other regions in the image.

2.2 NORMALIZATION

Once the iris region is successfully segmented from an eye image, the next stage is to transform the iris region so that it has fixed dimensions in order to allow comparisons. The dimensional inconsistencies between eye images are mainly due to the stretching of the iris caused by pupil dilation from varying levels of illumination. Other sources of inconsistency include, varying imaging distance, rotation of the camera, head tilt, and rotation of the eye within the eye socket. The normalization process will produce iris regions, which have the same constant dimensions, so that two photographs of the same iris under different conditions will have characteristic features at the same spatial location.

Another point of note is that the pupil region is not always concentric within the iris region, and is usually slightly nasal [2].This must be taken into account if trying to normalize the 'doughnut' shaped iris region to have constant radius.

2.2.1 Daugman's RubberSheet Model

The homogenous rubber sheet model devised by Daugman [1, 2] remaps each point within the iris region to a pair of polar coordinates (r,θ) where r is on the interval $[0,1]$ and θ is angle $[0,2\pi]$.

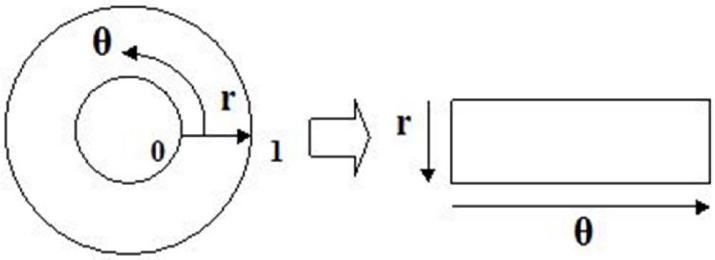

Figure 2-1 Daugman's Rubber Sheet Model

The remapping of the iris region from Cartesian coordinates (u,v) to the normalized non-concentric polar representation is modeled as:

$$I\left(u(r,\theta),\mathrm{v}(r,\theta)\right)\rightarrow I(r,\theta) \tag{9}$$

Where

$$u(r,\theta) = (1-r)u_p(\theta) + ru_i(\theta) \tag{10}$$

$$v(r,\theta) = (1-r)v_p(\theta) + rv_i(\theta) \tag{11}$$

The $I(\mathrm{u},\mathrm{v})$ is the iris image, (u,v) are the original Cartesian coordinates, (r,θ) are the corresponding normalized polar coordinates, and u_p, v_p and u_i, v_i are the coordinates of the pupil and iris boundaries along the θ direction.

The rubber sheet model takes into account pupil dilation and size inconsistencies in order to produce a normalized representation with constant dimensions. In this way the iris region is modeled as a flexible rubber sheet anchored at the iris boundary with the pupil center as the reference point.

Even though the homogenous rubber sheet model accounts for pupil dilation, imaging distance and non-concentric pupil displacement, it does not compensate for rotational inconsistencies. In the Daugman system, rotation is accounted for during matching by shifting the iris templates in the θ direction until two iris templates are aligned.

2.2.2 Image Registration

The Wildes et al. system employs an image registration technique, which geometrically warps a newly acquired image, $I_a(x,y)$ into alignment with a selected database image $I_d(x,y)$. When choosing a mapping function $(u(x,y), v(x,y))$ to transform the original coordinates, the image intensity values of the new image are made to be close to those of corresponding points in the reference image. The mapping function must be chosen so as to minimize

$$\int_x \int_y \left(I_d(x,y) - I_a(x-u, y-v)\right)^2 dxdy \tag{12}$$

while being constrained to capture a similarity transformation of image coordinates (x,y) to (x',y'), that is

$$\begin{pmatrix} x' \\ y' \end{pmatrix} = \begin{pmatrix} x \\ y \end{pmatrix} - sR(\phi)\begin{pmatrix} x \\ y \end{pmatrix} \tag{13}$$

with s a scaling factor and $R(\phi)$ a matrix representing rotation by ϕ. In implementation, given a

pair of iris images I_a and I_d, the warping parameters s and ϕ are recovered via an iterative minimization procedure.

2.2.3 Virtual Circles

In the Boles system, iris images are first scaled to have constant diameter so that when comparing two images, one is considered as the reference image. This works differently to the other techniques, since normalization is not performed until attempting to match two iris regions, rather than performing normalization and saving the result for later comparisons. Once the two irises have the same dimensions, features are extracted from the iris region by storing the intensity values along virtual concentric circles, with origin at the center of the pupil. A normalization resolution is selected, so that the number of data points extracted from each iris is the same. This is essentially the same as Daugman's rubber sheet model; however scaling is at match time, and is relative to the comparing iris region, rather than scaling to some constant dimensions. Also, it is not mentioned by Boles, how rotational invariance is obtained.

2.3 FEATURE ENCODING

In order to provide accurate recognition of individuals, the most discriminating information present in an iris pattern must be extracted. Only the significant features of the iris must be encoded so that comparisons between templates can be made.

2.3.1 Wavelet Encoding

Wavelets can be used to decompose the data in the iris region into components that appear at different resolutions. Wavelets have the advantage over traditional Fourier transform in that the frequency data is localized, allowing features which occur at the same position and resolution to be matched up. A number of wavelet filters, also called a bank of wavelets, is applied to the 2D iris region, one for each resolution with each wavelet a scaled version of some basis function. The output of applying the wavelets is then encoded in order to provide a compact and discriminating representation of the iris pattern.

2.3.2 Gabor Filters

Gabor filters are able to provide optimum conjoint representation of a signal in space and spatial frequency. A Gabor filter is constructed by modulating a sine/cosine wave with a Gaussian. This is able to provide the optimum conjoint localization in both space and frequency, since a sine wave is perfectly localized in frequency, but not localized in space. Modulation of the sine with a Gaussian provides localization in space, though with loss of localization in frequency. Decomposition of a signal is accomplished using a quadrature pair of Gabor filters, with a real part specified by a cosine modulated by a Gaussian, and an imaginary part specified by a sine modulated by a Gaussian. The real and imaginary filters are also known as the even symmetric and odd symmetric components respectively.

The center frequency of the filter is specified by the frequency of the sine/cosine wave, and the bandwidth of the filter is specified by the width of the Gaussian. A 2D Gabor filter over the image domain (u,v) is represented as:

$$g(\mathrm{u},\mathrm{v}) = e^{-\pi\left[(u-u_o)^2/\delta^2+(v-v_o)^2/\kappa^2\right]} e^{-2\pi i\left[p_o(u-u_o)+q_o(v-v_o)\right]} \tag{14}$$

Where (u_o,v_o) specify position in the image, (δ,κ) specify the effective width and length, and (p_o,q_o) specify modulation, which has spatial frequency $\varpi_o = \sqrt{{p_o}^2+{q_o}^2}$.

2.3.3 Haar Wavelet

Limet al. also use the wavelet transform to extract features from the iris region. Both the Gabor transform and the Haar wavelet are considered as the mother wavelet. From multi-dimensionally filtering, a feature vector with 87dimensions is computed. Since each dimension has a real value ranging from -1.0 to +1.0, the feature vector is sign quantized so that any positive value is represented by 1 and negative value as 0. This results in a compact biometric template consisting of only 87 bits.

Limet al. compare the use of Gabor transform and Haar wavelet transform, and show that the recognition rate of Haar wavelet transform is slightly better than Gabor transform by 0.9%.

2.3.4 Laplacian of Gaussian Filters

In order to encode features, the Wildes etal. System decomposes the iris region by application of Laplacian of Gaussian filters to the iris region image. The filters are given as

$$\nabla G = -\frac{1}{\pi\sigma^4}\left(1-\frac{\rho^2}{2\sigma^2}\right)e^{-\rho^2/2\sigma^2} \tag{15}$$

Where σ is the standard deviation of the Gaussian and ρ is the radial distance of a point from the center of the filter.

The filtered image is represented as a Laplacian pyramid which is able to compress the data, so that only significant data remains. Details of Laplacian Pyramids are presented by Burt and Adelson. A Laplacian pyramid is constructed with four different resolution levels in order to generate a compact iris template.

2.4 FEATURE MATCHING

The template that is generated in the feature encoding process will also need a corresponding matching metric, which gives a measure of similarity between two iris templates. This metric should give one range of values when comparing templates generated from the same eye, known as intra-class comparisons, and another range of values when comparing templates created from different irises, known as inter-class comparisons. These two cases should give distinct and separate values, so that a decision can be made with high confidence as to whether two templates are from the same iris, or from two different irises.

2.4.1 Hamming distance

The Hamming distance gives a measure of how many bits are the same between two bit patterns. Using the Hamming distance of two bit patterns, a decision can be made as to whether the two patterns were generated from different irises or from the same one. In comparing the bit patterns X and Y, the Hamming distance, HD, is defined as the sum of disagreeing bits (sum of the exclusive-OR between X and Y) over N, the total number of bits in the bit pattern.

$$HD = \frac{1}{N}\sum_{j=1}^{N} X_j \otimes Y_j \tag{16}$$

Since an individual iris region contains features with high degrees of freedom, each iris region will produce a bit-pattern which is independent to that produced by another iris, on the other hand, two iris codes produced from the same iris will be highly correlated.

If two bits patterns are completely independent, such as iris templates generated from different irises, the Hamming distance between the two patterns should equal 0.5.This occurs because independence implies the two bit patterns will be totally random, so there is 0.5 chance of setting any bit to 1,and vice versa. Therefore, half of the bits will agree and half will disagree between the two patterns. If two patterns are derived from the same iris, the Hamming distance between them will be close to 0.0, since they are highly correlated and the bits should agree between the two iris codes.

The Hamming distance is the matching metric employed by Daugman, and calculation of the Hamming distance is taken only with bits that are generated from the actual iris region.

2.4.2 Weighted Euclidean Distance

The weighted Euclidean distance (WED) can be used to compare two templates, especially if the template is composed of integer values. The WED gives a measure of how similar a collection of values are between two templates. This metric is employed by Zhu et al. and is specified as

$$WED(k) = \sum_{i=1}^{N} \frac{\left(f_i - f_i^{(k)}\right)^2}{\left(\delta_i^{(k)}\right)^2} \tag{17}$$

Where f_i is the i^{th} feature of the unknown iris, and $f_i^{(k)}$ is the i^{th} feature of iris template, k and $\delta_i^{(k)}$ is the standard deviation of the i^{th} feature in iris template k. The unknown iris template is found to match iris template k, when WED is a minimum at k.

2.4.3 Normalized Correlation

Wildes et al. make use of normalized correlation between the acquired and database representation for goodness of match. This is represented as

$$\frac{\sum_{i=1}^{n}\sum_{j=1}^{m}\left(p_1[i,j]-\mu_1\right)\left(p_2[i,j]-\mu_2\right)}{nm\sigma_1\sigma_2} \tag{18}$$

Where p_1 and p_2 are two images of size $n \times m$, μ_1 and σ_1 are the mean and standard deviation of p_1, and, μ_2 and σ_2 are the mean and standard deviation of p_2.

Normalized correlation is advantageous over standard correlation, since it is able to account for local variations in image intensity that corrupt the standard correlation calculation.

CHAPTER 3
PROPOSED METHODOLOGY

First an eye image is captured and converted to a digital form to make it suitable for analysis. In the proposed work as soon as the input image is fed into the system, histogram equalization is applied to it. This will enhance the contrast of the dark regions of the image and improves its equalization. Iris regions in gray scale images are generally at the darker side and to clearly analyze such regions this modification is very beneficial. This will lead to more accurate segmentation and hence more accurate rejection and acceptance rates.

Next, the doughnut like iris section of the eye image must be determined. After defining it accurately it should be isolated from the digital image so that further processing can be done on the desired area. This isolation of the iris portion i.e. segmentation of iris region is performed in two steps. In the first step, the inner and outer boundaries of iris are isolated by using Integro-Differential operator [1] and in the second step the eyelids, specular highlights, eyelashes and other noise components are detected by using parabolic Hough Transform technique.

3.1 ISOLATING IRIS PORTION USING INTEGRO-DIFFERENTIAL OPERATOR

The problem of finding the pupil boundary or iris inner boundary can be seen as an optimization issue. In this problem, a sequence of circles with increasing radii in a range is taken. These circles are then placed on a grid. The center coordinates of such circles are located at one of a number of trial points on that grid. Mathematically, to represent such series of circles a range of radii is provided to the system and the impact of this range of radii is discussed in the Sub-topic 3.4. On each of these circles a fixed number of points are taken. Next, the summation of the brightness of image on each of these points is calculated. Though, here 128 points are used irrespective of increasing radii, to avoid automatic increase in the summed brightness. Now as radius increases, we calculate the summation of the image brightness for each of such circles and iteratively check for the maximum rate-of-change in this quantity. A sudden change or spike in this value shows the best candidate circle with papillary boundary. In this optimization problem

of locating papillary boundary, it is searched for a three-parameter space, i.e. the best possible composition of circle center coordinates (u_o, v_o) and radius r .

Mathematically it is described, as in equation (7), as summation of the image intensity $I(\mathrm{u},\mathrm{v})$ over the arc (ds) of a circle. The radius of the circle taken is r and its center coordinates are (u_o, v_o). Then partial derivative of this quantity is computed with respect to r with increasing radii. As described above, next it is searched over a three-parameter space (u_o, v_o, r) for the maximum absolute value of this partial derivative. The partial derivative with respect to r is convoluted $(*)$ with a smoothing function $G_\sigma(r)$ to enhance noise immunity. In effect, the Integro-Differential operator actually behaves as a circular edge detector.

Although it is described mathematically but to implement this operator the order of convolution and differentiation is interchanged. To make it efficient before computing the discrete convolution of the resulting operator, concatenation is performed with the discrete series of pixels (using a constant value, 128) along each of the circles with increasing radii. This approximation is given as:

$$\frac{\partial G_\sigma(r)}{\partial r} \approx G_\sigma{}^{(1)}(n) = \frac{1}{\Delta r} G_\sigma(n\Delta r) - \frac{1}{\Delta r} G_\sigma\left((n-1)\Delta r\right) \tag{19}$$

Where Δr is a difference in two radii, and when convolution and contour integrals are replaced with sums, an efficient operator is derived (see (3.3) below) for finding the inner and outer boundaries of the iris.

$$\max_{(n\Delta r, \mathrm{u}_o, \mathrm{v}_o)} \left| \frac{1}{\Delta r} \sum_k \left\{ \left(G_\sigma\left((n-k)\Delta r\right) - G_\sigma\left((n-k-1)\Delta r\right) \right) \sum_m I\left[\left(k\Delta r \cos(m\Delta\theta) + u_o\right), \left(k\Delta r \sin(m\Delta\theta) + v_o\right) \right] \right\} \right| \tag{20}$$

Where $\Delta\theta$ is the angle formed at the center of circle by the sides (600 sided polygon is used in this work to use constant number of points on each circle) of the polygon taken, next it is summed over the $I(\mathrm{u},\mathrm{v})$ pixel intensities which represents the contour integrals as expressed in equation (7).

3.2 DETECTING NOISE ELEMENTS USING HOUGH TRANSFORM

In the present work above algorithm only segments out the region of interest but the occluding elements are removed by the Hough transform technique [3]. The standard Hough transform algorithm can be used to determine the simple geometric objects present in an image. These objects may be lines, circles, arcs, etc. In this paper, the upper and lower eyelids are approximated with parabolic arcs using parabolic Hough transform and are represented as in equation (6).

To detect eyelids which are usually horizontally aligned, horizontal directed derivatives are applied. Hence the overall segmentation of iris region is performed in two steps here.

3.3 A COMBINATION OF INTEGRO-DIFFERENTIAL OPERATOR AND HOUGH TRANSFORM

The Integro-Differential Operator and Hough transform are somewhat related. Integro-Differential also performs a search in n-parameter space by making use of first derivatives of the image to find geometric objects. The thresholding problems are not involved in it, since it makes use of the raw derivative information. On the other hand Hough transform method requires choosing of threshold values for edge detection and due to this; sometimes critical edge points get removed. This may result in failure to detect circles. So, we make use of the Integro-Differential operator to isolate the iris portion. However, this algorithm, since it works only on a local scale, sometimes cannot work when noise is present in the eye image, such as from reflections. Hence, to encounter such noise factors we make use of the Hough Transform in the next step. It is so because the Hough transform uses 'brute-force' approach and is computationally intensive. These two steps together significantly improve the segmentation of the iris region. An accurate segmentation is very crucial as this result will directly affect the later stages of iris processing and which will directly improve the false rejection and false acceptance rates of the system.

3.4 A NEW RANGE OF RADII

In this system a range of radii is used to search for the iris and pupil circles in the image. This range is provided to the already defined Integro-differential operator as an input, in which a

series of circles with increasing radii are searched for the best candidate for limbic and pupillary boundaries. Such range is reduced from [80-150] (used in Libor Masek's System) to [95-110] in the system. This change in range of radii is proposed on the basis of the experimental results as shown in the next Section. Systems, with ranges as mentioned above, are applied to 115 users' eye images and it is found that results from both the systems, i.e. the system with [80-150] as range of radii and the system with [95-110] as range of radii, are similar. Since the necessary region of the image is covered in this range of radii, the overall efficiency of the system is maintained. And instead of searching for all possible radii in the range, which would require a lot of time, only an optimal range of radii is searched for finding the boundaries and it results in reduction of the overall time complexity of the system.

3.5 SCALING FACTOR

The scaling factor reduces the size of the image before it is processed for finding the pupil and iris boundaries. Next, based on this scaled image, iris and pupil boundaries are found and then the image is again recovered back to its original size. The scaling factor used in this work is 0.25, i.e. the size of the image is reduced by 75% of the original size, instead of 0.40 (as used by Labor Masek [3]). Due to this, the number of comparisons made to find out the boundaries of iris region is drastically reduced. This helps in reducing the time complexity of the overall system while maintaining the accuracy level.

3.6 POWER LAW FUNCTION

To enhance darker region of images the power law transformation (gamma function) is applied with constant gamma value $\gamma = 2.5$. This is applied to the image after iris region is isolated but before noise areas are detected by the system. After applying this gamma function, various noise elements like eyelids, eyelashes, specular highlights, etc. can be easily occluded from the image using parabolic hough transform. The mathematical formula of gamma function is as follows:

$$y = x^{1/\gamma} \tag{21}$$

Where x = Original image intensity matrix,

y = New image intensity matrix obtained,

γ = Constant.

The reason of using this function is as follows. Here the noise elements around the boundary of iris region are searched. They have generally low intensity pixels as compared to the iris region. But some areas inside the iris region can also have this property. The image is enhanced with gamma function so that the system do not consider actual iris region as noise elements. Wherever such an area is found its intensity is changed to $Null$. In formula (21), if $\gamma > 1$ is used, the image will be shifted to the brighter side and if $\gamma < 1$ is used the image will be shifted to the darker side. As we are using the value of γ = 2.5, the image will be shifted more to the brighter side but up to a certain limit.

3.7 IRIS NORMALIZATION BASED ON DAUGMAN'S RUBBER SHEET MODEL

The iris portion of the image is defined and isolated now. To produce an iris code, this defined area must be analyzed. In order to allow comparisons, this stage will transform the iris region into a region that will have fixed dimensions. Due to the varying levels of illumination pupil gets dilated or contracted and hence stretching of the iris is caused. Due to this stretching various inconsistencies arise at the dimensional level in the eye images. Inconsistency also arises due to many other reasons, including: 1) taking image from different distances, 2) camera rotation, 3) tilting of head and 4) rotation of the eye within the eye socket. The iris pattern should be represented in a way that must be resistant to any changes in size, position and it also must be invariant to the orientation of the patterns and this stage focuses to produce iris regions that follow these requirements. It should produce the same constant dimensions so that if we take two photographs of the same iris under different environments then the characteristic features of these two images must be at the same spatial location.

In other words, approximately the same iris code should be generated from the same iris in its different states of pupillary dilation. By using the dimensionless coordinate system as suggested above, various distortions get eliminated. In this system, total distance from iris inner boundary to outer boundary is divided into a number of fractions and these fractions are used to mark off the total distance.

Another point of note is that the pupil and iris regions are not always concentric. Very often the pupil center is nasal, and inferior, to the iris center [8]. Also there is an estimate that the radius of the pupil can range from 0.1 to 0.8 of the iris radius. Thus, all three parameters i.e. the center coordinates and radius of pupillary circle must be determined separately from those of the iris.

In the Daugman's homogenous rubber sheet model [2], as shown in figure (2-1), each point within the iris region is remapped to a pair of polar coordinates (r,θ) where r is on the interval $[0,1]$ and θ is angle $[0,2\pi]$. The remapping of the iris region from Cartesian coordinates (u,v) to the normalized non-concentric polar representation is depicted in equations (9), (10) and (11).

Hence, by taking pupil center as the reference point, the iris region is modeled as a flexible rubber sheet attached at the iris boundary. This model does not account for the rotational inconsistencies. This inconsistency regarding the rotation is accounted during matching phase. To do so the iris templates are shifted in the θ direction until two iris templates get aligned.

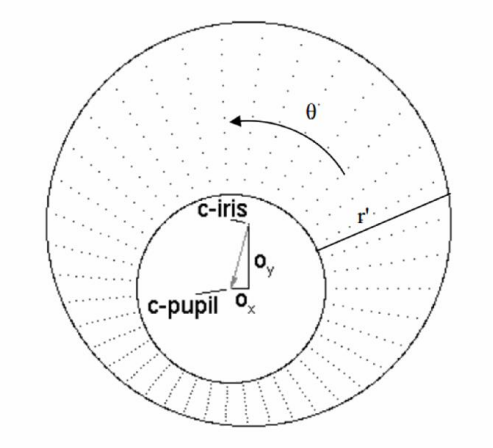

Figure 3-1 Normalization process with angular and radial resolution (Pupil displacement relative to the iris center is exaggerated)

Proposed work uses a technique based on Daugman's Rubber Sheet Model for normalization. The pupil's center is taken as the reference point and radial vectors pass through the iris region, as shown in Figure 5. A fixed number of points are selected along each radial line and this is defined as the radial resolution whereas the number of radial lines going through the iris region is defined as the angular resolution.

To account for the non-concentric nature of the pupil and iris centers, and to rescale points a remapping formula is needed and is given as:

$$r' = \sqrt{\delta}\kappa \pm \sqrt{\delta\kappa^2 - \delta - r_j^2} \tag{22}$$

Where

$$\delta = \omega_x^2 + \omega_y^2 \tag{23}$$

$$\kappa = \cos\left(\pi - \arctan\left(\frac{\omega_y}{\omega_x}\right) - \theta\right) \tag{24}$$

The ω_x, ω_y represents the displacement of the center of the pupil relative to the center of the iris, r' is the distance between the edges of the pupil and iris at an angle, θ around the region, and r_j is the radius of the iris. This remapping formula gives the radius of the doughnut shaped iris region as a function of the angle θ.

3.8 FEATURE ENCODING USING LOG-GABOR FILTER

To make comparisons between templates, encoding of the significant features of the iris must be done. For perfect localization it is required to access the space and frequency domains separately. Such requirement is fulfilled by Gabor filters which are constructed by modulating a sine/cosine wave with a Gaussian. Modulating sine wave with a Gaussian results in localization in space but with the loss of localization in frequency. A quadrature pair of Gabor filter is used to decompose the signal. Cosine wave modulated by a Gaussian specifies a real part and a sine modulated by a Gaussian specifies an imaginary part. These real and imaginary filters are also known as the even symmetric and odd symmetric components respectively. Where frequency of the sine/cosine wave is used as the center frequency of the filter and bandwidth of the filter is used as the width of the Gaussian.

It has been shown by Oppenheim and Lim [15] that the most significant information within an image is provided by the phase information rather than the amplitude information. Hence encoding of this phase information will results in encoding of the discriminating features of iris. A Gabor filter over an image domain (u, v) is represented as in equation (14).

The odd and even symmetric Gabor filters are shown in Figure 3-2. To demodulate the output of the Gabor filters, the phase information is quantized into four levels, with each level for each possible quadrant in the complex plane. Two bits of data are required to represent these four levels.

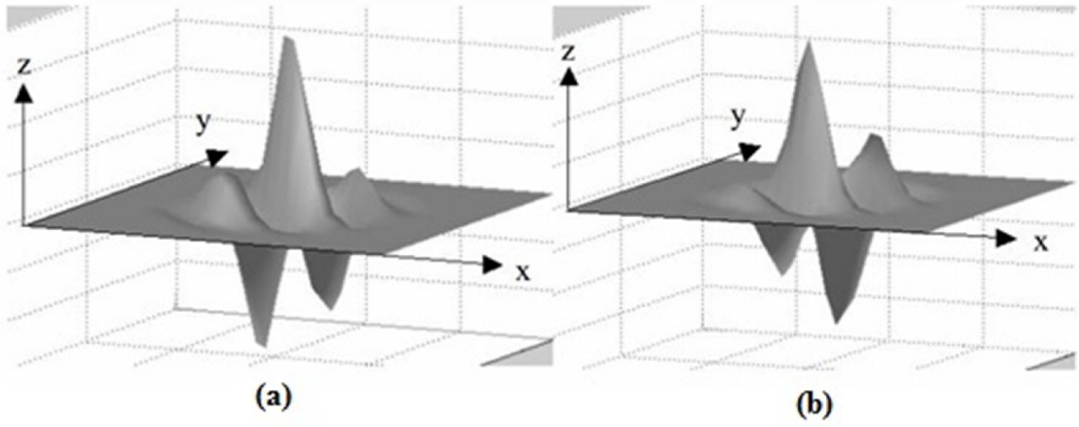

Figure 3-2 A quadrature pair of 2D Gabor filters a) real component or even symmetric filter b) imaginary component or odd symmetric filter

Hence, in the iris code two bits of data are used for each pixel. A total of 2,048 bits are generated for the template, and 2,048 masking bits are also generated to create the mask matrix of each iris region. This mask is used to indicate and to mask out corrupted regions within the iris. This process creates a compact 256-byte template that allows for efficient storage and comparison of irises.

After broking the 2D normalized iris pattern into a number of 1D signals it is convolved with 1D Gabor wavelets. Here each row or each circular ring is taken as the 1D signal. Using Daugman method [5], the obtained output of filtering is phase quantized into four levels, with each filter for each phasor produces two bits of data. The phase-quadrant demodulation is depicted as in Figure 3-3.

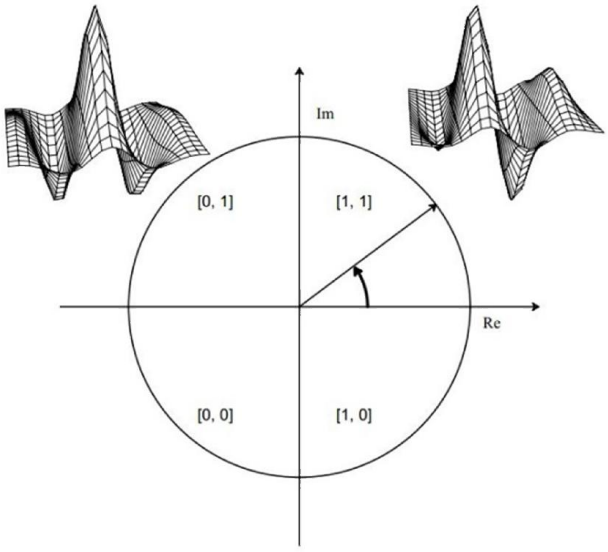

Figure 3-3 A quadrature pair of 2D Gabor filter

Phase quantization is so well performed that if we have to go from one quadrant to other, only one bit of data changes and it helps in minimizing the number of bits disagreeing. During the encoding process noise areas in the normalized pattern are also set to the average intensity of some neighborhood pixels so that filters can be applied smoothly and no noise area can influence the output of the filters. Overall encoding process will produces a bitwise template containing information and a corresponding noise mask to represent the corrupt areas within the iris pattern.

3.9 FEATURE MATCHING USING HAMMING DISTANCE

To decide among the templates a matching metric is needed that will give a measure of similarity between two iris templates. This metric should be defined in a manner that for intra-class comparisons it uses one range of values, and for inter-class comparisons another range of value is used. This will surely help in making a decision with high confidence about two templates, i.e. they are from the same iris, or from two different irises.

For such classification of iris templates, the Hamming distance is employed, and two templates are said to match if a test of statistical independence is failed. As it involves constant length of the iris codes and a format that is universally acceptable, comparisons between them are readily implemented by the Exclusive-OR (XOR) logical operation [1], [9]. The system performed perfect authentication on a set of 115 standard eye images of CASIA-IrisV4-Sync database. To

handle the rotational inconsistencies of the iris, a pair of templates is compared by rotating one template over the other. And the range of rotations is taken to be [(-2)-2]. The formula to calculate hamming distance (d) or the XOR comparison of two irises codes is as follows:

$$d = \frac{\left\| \left(c_A \otimes c_B \right) \cap m_A \cap m_B \right\|}{\left\| m_A \cap m_B \right\|} \tag{25}$$

Where, c_A = Iris Code of template A

c_B = Iris Code of template B

m_A = Mask of template A

m_B = Mask of template B

Finally, the best result is chosen from many results obtained by rotating one template over the other. This process removes inconsistencies but at the same time increases the time complexity of the system. So, the rotation of the templates if limited to a certain number gives reasonable results within reasonable time and therefore the number of rotations (and hence comparisons) are reduced.

CHAPTER 4
EXPERIMENTAL RESULTS

Various tests were carried out on the proposed system and on the system developed by Masek to examine the performance of both the systems. IRS provided by Masek was able to produce effective recognition rates. However, results published by him, were majorly produced under favorable conditions. The proposed work provides an enhancement over Libor Masek's work in terms of time complexity as well as in false acceptance and rejection rates.

All time complexities shown in this paper are for 52900 comparisons carried out on 115 users' eyes database, with 2 images per user, taken from CASIA-IrisV4-Sync database. Also the False Acceptance Rates (FARs) and False Rejection Rates (FRRs) are calculated by taking decision criteria at a hamming distance of 0.3.

4.1 IMAGE ENHANCEMENT USING HISTOGRAM EQUALIZATION

First any image passed to the proposed system is Histogram Equalized. The effect of this operation is shown in Figure 4-1.

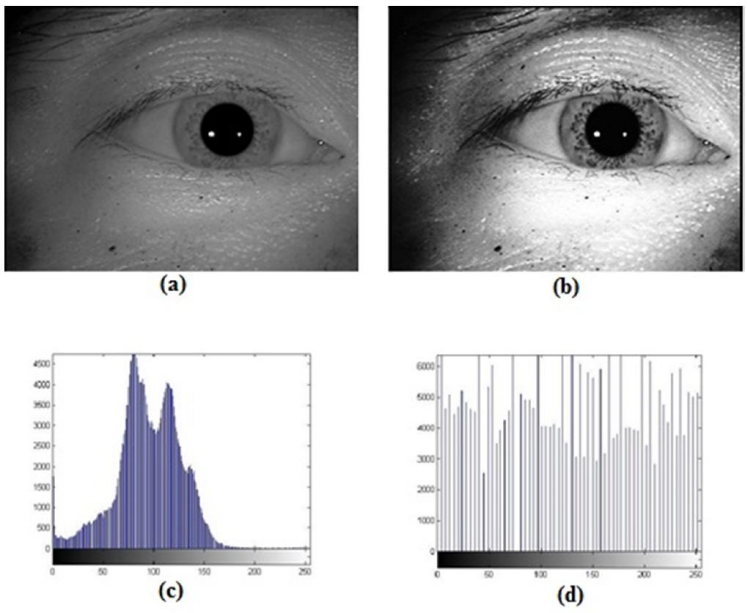

Figure 4-1 Image enhancement using histogram equalization (a) Original image, (b) Enhanced image, (c) Histogram of the original image and (d) Histogram of the enhanced image

The iris portion of the eye is usually not clear and from Figure 4-1 it can be seen that the iris portion of original image (top-left) is not visible but after applying histogram equalization to the image (top-right), this region is clearly visible. This is achieved because this operation enhances the contrast of the image and makes its pixels to span along the whole levels. This can be verified by their histograms (bottom-left and bottom-right) as shown in Figure 4-1.

4.2 ERROR REDUCTION IN SEGMENTATION PHASE

The number of images with improper segmented iris region got reduced in the proposed work due to the use of a mix of Integro-Differential Operator and Hough transform. An image must be segmented properly as this is the crucial step in error reduction, otherwise this error will increase exponentially in the later stages. An image with its segmented counterparts by both methods is as shown in Figure 4-2. A random image (left) is segmented by using Masek's work (middle) and by the proposed work (right) and it can be seen from Figure 4-2 that the proposed method isolates the iris region properly but Masek's work fails to isolate the iris region properly on the same image.

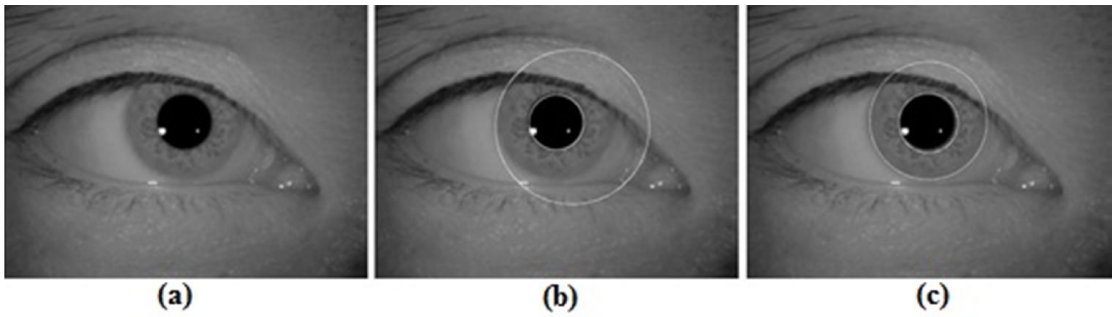

Figure 4-2 (a) A random image from CASIA sync database, (b) Iris region isolated by using Masek's work, (c) Iris region

Further, a range of standard CASIA images has been used to test this work against Masek's method and proposed method as shown in Table 2. By implementing Libor Masek's work on a dataset of 230 images, 35 images were found which are not segmented properly, i.e. an error-rate of 15.22% is detected. Also, by implementing the proposed work on the same dataset of 230 images, only 4 such images were found, i.e. an error-rate of 1.74% is detected. The error-rate is reduced from 15.22% to 1.74% and hence, there is an overall error reduction of 88.57% is found in the iris segmentation phase.

Table 4-1 Comparison of the Error-rates in segmentation phase. A dataset of 230 images is used

Method	Images with properly isolated iris region	Images with improper isolated iris region	Error-Rate in isolating iris region
Libor Masek's Method	195	35	15.22%
Proposed Method	226	4	1.74%

4.3 TIME COMPLEXITY REDUCTION DUE TO RANGE OF RADII

As described in Sub-topic 3.4, range of radii is reduced from [80-150] to [95-110] in the proposed work. Error-rates and time complexities for both these ranges against Masek's method and proposed method are shown in Table 4-2.

Table 4-2 Comparison in terms of FAR, FRR and Time complexity when range of radii is changed

Method	FAR	FRR	Time Complexity (sec)
Libor Masek's Method	11.751%	13.913%	17622.02
Proposed Method with range of radii [80-150]	0.458%	0.87%	16680.17
Proposed Method with range of radii [90-115]	0.488%	0.87%	12197.14

From Table 4-2, it can be seen that FRR remains same for the two cases of proposed work, but FAR improves slightly by a factor of 0.030 when the range of radii increases. At the same time its turnaround time increases from 12197 seconds to 16680 seconds i.e., an increment of the order of 26.92% is depicted. Hence reduction in range of radii helps in improvement of the time complexity but over reduction of range will lead to high error-rates.

4.4 POWER LAW FUNCTION

As described in Sub-topic 3.6 Power Law Function or Gamma Function is applied before the second step of the segmentation phase. This will enhance the darker regions of the iris to help in better noise detection.

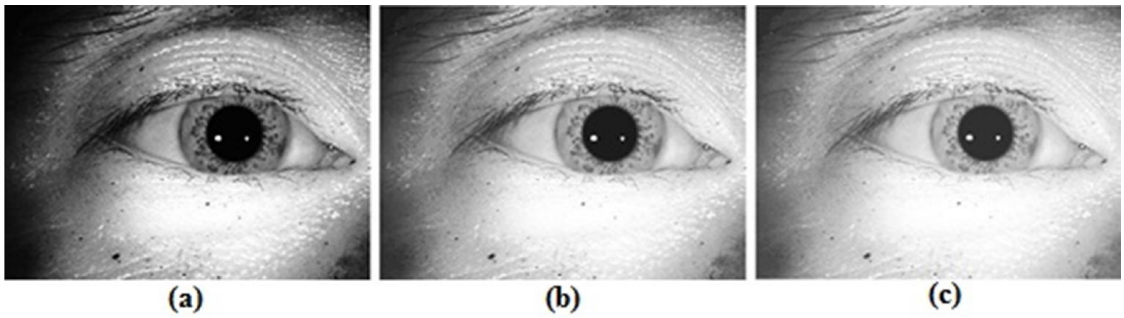

Figure 4-3 Power Law Function applied on histogram equalized image (a), with gamma value 1.9 used in Libor Masek's method (b) and with gamma value 2.5 used in the proposed work (c)

The gamma function is applied on histogram equalized image and Figure 4-3 shows the resultant images with gamma constant values 1.9 (middle) and 2.5 (right) in Libor Masek's and proposed work respectively.

4.5 SCALING FACTOR

In the proposed work the image is scaled by a factor of 0.25 instead of 0.4 as used in Masek's work. Scaling down an image will directly reduce the time complexity of the system as it will require the less number of comparisons for the same image as against the comparisons required for the non-scaled image. Also more you scale down the image more time can be saved but at the same time this will compromise with the details of the image and hence compromise with the error rates produced by the system.

Table 4-3 Comparison in terms of FAR, FRR and Time complexity when scaling factor is changed against Masek's method and proposed method

Method	FAR	FRR	Time Complexity (sec)
Libor Masek's Method (scaling factor 0.4)	11.751%	13.913%	17633.02
Proposed Method (with scaling factor 0.4)	0.438%	0.87%	17460.96
Proposed Method (with scaling factor 0.25)	0.488%	0.87%	12197.14

So scaling must be done up to a certain limit through which error rates are found to be similar. This comparison of results is as shown in Table 4-3 keeping all other factors constant.

Table 4-3 shows that FRR remains same for the two cases of proposed work, though FAR improves by 0.05 when scaling factor increases, but at the same time its time complexity increases from 12190 seconds to 17460 seconds i.e. an increment of the order of 30.18% is shown by the system. Reduction in scaling factor improves the time complexity however; if scaling factor is reduced more than a limit then error-rates of the system will be so high that it makes the authentication unreliable.

4.6 NUMBER OF ROTATIONS DURING TEMPLATE MATCHING

Template matching by Hamming Distance technique gives us the result in the range of [0-1]. But the rotational inconsistencies are needed to be dealt with and hence we rotate one template over the other as described in Sub-topics 2.4 and 3.9. The number of rotations is to be selected carefully. In the proposed work we reduce the number of rotations from [(-8)-8] (used in Masek's work) to [(-2)-2]. The improvement in results due to reduction in number of rotations is shown in Table 4-4.

Table 4-4 Comparison in terms of FAR, FRR and Time complexity when number of rotations is changed

Method	FAR	FRR	Time Complexity (sec)
Libor Masek's Method	11.751%	13.913%	17622.02
Proposed Method with [(-8)-8] Rotations	0.448%	0.87%	16460.96
Proposed work with [(-2)-2] Rotations	0.488%	0.87%	12197.14

We have experimented with a range of standard images and noticed a considerable saving in computation time by reducing the number of iterations without losing the quality. From Table 4-4 it can be seen that FRR remains same for the two cases of proposed work, though FAR again improves by 0.04 when range of rotation increases. At the same time the time complexity of the system is increased from 12190 seconds to 16460 seconds i.e. an increment in the order of

25.94% is shown by the system. Hence reduction in range of rotations helps to improve the time complexity but over reduction of range of rotations will lead to high error-rates.

4.7 OVERALL FAR, FRR AND TIME COMPLEXITY OF THE PROPOSED SYSTEM

After incorporating all of the above modifications, the final proposed system when implemented showed the results as depicted by the Table 4-5. From Table 4-5, it can be seen that the proposed system performs better than Masek's system. The FAR of the proposed system and Masek's system are 0.488% and 11.750% respectively, i.e. an improvement of 95.85% is obtained in False Acceptance Rate.

Table 4-5 Overall comparisons in terms of FAR and FRR and Time complexity among Masek's and Proposed work

Method	FAR	FRR	Time Complexity (sec)
Libor Masek's Method	11.75057%	13.91304%	17622.02
Proposed Method	0.488177%	0.869565%	12197.14

Now, the FRR of the proposed system and Masek's system are found to be 0.869% and 13.913% respectively, i.e. an improvement of 93.75% is obtained in False Rejection Rate. Also, the turnaround time reduces from 17622 seconds to 12197 seconds in the proposed system. It shows an improvement of the order of 30.79% in Time complexity by the proposed system against the Masek's system.

CHAPTER 5
CONCLUSION

The proposed method can be used to recognize individuals as confirmed by the experimental results. Various conclusions can be drawn from this work. These are:

a) In the pre-processing stage use of histogram equalization operation enhances the digital image and this directly helps in all other later stages of the system.
b) The use of a mix of Integro-Differential Operator and Hough Transform isolates the iris region accurately. Major portion of the improvement in error-rates is achieved by this technique.
c) A new range of radii to the system helps in reduction of system's Time complexity.
d) Use of Power Law Function with new gamma value helps in drawing a line between noisy areas and iris region more accurately.
e) Scaling down an image directly reduces the Time complexity of the system.
f) Number of times a template is rotated over the other and each time a hamming distance is calculated to find out the possibility of matching two irises of the same person in different conditions is also reduced. This will check out for the rotational inconsistencies and reduces the Time complexity of the system.

Due to the various changes and modifications proposed in the Labor Masek's work the Time complexity of the system is reduced by 31% approximately. Also, the False Rejection and False Acceptance Rates are improved by 93.75% and 95.85% respectively. Hence this system is a more powerful candidate to be used in real-time applications.

BIBLIOGRAPHY

[1] Daugman, J., “Biometric Personal Identification System Based on Iris Analysis”, US005291560A.

[2] Daugman, J., “How Iris Recognition Works”, IEEE Transactions on Circuits and Systems, Vol. 14, No.1, January 2004.

[3] Masek, L., “Recognition of Human Iris Patterns for Biometric Identification”, University of Western Australia, 2003.

[4] http://www.sinobiometrics.com, “Chinese Academy of Sciences Institute of Automation, CASIA-IrisV4 Database”.

[5] Daugman, J., “Recognizing Persons by their Iris Patterns”, Cambridge University, U.K.

[6] Daugman, J., “New Methods in Iris Recognition”, IEEE Transactions on Systems, Man, and Cybernetics—Part B: Cybernetics, Vol. 37, No. 5, October 2007.

[7] Daugman, J., Dowing, C., "Epigenetic Randomness, Complexity, and Singularity of Human Iris Patterns”, In: Preceding soft the Royal Society, B, 268, Biological Sciences, pp.1737–1740(2001).

[8] Daugman, J., “Statistical richness of visual phase information: update on recognizing Persons by iris patterns”, Int. J. Comput.Vis., 45(1), 25–38(2001).

[9] Daugman, J., “High Confidence Visual Recognition of Persons by a Test of Statistical Independence”, IEEE Transactions on Pattern Analysis and Machine Intelligence, Vol. 15, No. 11, November1993.

[10] Daugman, J., “Probing the Uniqueness and Randomness of IrisCodes: Results From 200 Billion Iris Pair Comparisons”, Vol. 94, No. 11, November 2006, Proceedings of the IEEE.

[11] Daugman, J., “The Importance of Being Random: Statistical Principles of Iris Recognition”, The Journal of the Pattern Recognition Society, 2003, 279 – 291.

[12] Algirdas Bastys, "Iris Matching by Local Extremum Points of Multi scale Expansion", ICB2009, LNCS5558, pp.1070–1079, Springer-Verlag Berlin Heidelberg, 2009.

[13] Chouhan, B., Shukla, S., "Iris Recognition System using canny edge detection for Biometric Identification", International Journal of Engineering Sciences and Technology (IJEST), ISSN: 0975-5462 Vol. 3 No. I, Jan 2011.

[14] Yung-Hui Li, Marios Savvides, “An Automatic Iris Occlusion Estimation Method Based on High-Dimensional Density Estimation”, Vol. 35, No. 4, April 2013.

[15] ISO/IEC 19794-6:2005-06-01, “Information Technology- Biometric Data Interchange Formats- Part6: Iris image data”.

[16] A. Oppenheim J. Lim, “The importance of phase in signals”, Proceedings of the IEEE 69, 529-541, 1981.

[17] M. Vatsa, Department of CSE, IIT Kanpur, India; R. Singh, Department of CSE, IIT Kanpur, India; P. Gupta, Department of CSE, IIT Kanpur, India; “Comparison of Iris Recognition Algorithms”, IClSlP 2004.

[18] Ehsan M. Arvacheh, “A Study of Segmentation and Normalization for Iris Recognition Systems”, University of Waterloo, Ontario, Canada, 2006.

[19] S. V. Sheela, P. A. Vijaya, “Iris Recognition Methods - Survey”, International Journal of Computer Applications Volume 3 – No.5, June 2010.

[20] Surjeet Singh, Kulbir Singh, “Segmentation Techniques for Iris Recognition System”, International Journal of Scientific & Engineering Research Volume 2, Issue 4, April-2011.

[21] S. Jayalakshmi, Dr. M. Sundaresan, “A Survey on Iris Segmentation Methods”, 2013 International Conference on Pattern Recognition, Informatics and Mobile Engineering, February 21-22.

[22] Li Ma, Tieniu Tan, Yunhong Wang, Dexin Zhang, “Personal Identification Based on Iris Texture Analysis”, IEEE Transactions on Pattern Analysis and Machine Intelligence, Vol. 25, No. 12, December 2003.

[23] Mahboubeh S., Puteh S., Subariah I., Abdolreza K., “Fast Algorithm for Iris Localization Using Daugman Circular Integro Differential Operator”, International Conference of Soft Computing and Pattern Recognition, 2009.

[24] Karen P. Hollingsworth, Kevin W. Bowyer, Patrick J. Flynn, “The Best Bits in an Iris Code”, IEEE Transactions on Pattern Analysis and Machine Intelligence, Vol. 31, No. 6, June 2009.

[25] Wenbo Dong, Zhenan Sun,Member, IEEE; Tieniu Tan, Fellow, IEEE; “Iris Matching Based on Personalized Weight Map”, IEEE Transactions on Pattern Analysis and Machine Intelligence, Vol. 33, No. 9, September 2011.

[26] Khattab M. Ali Alheeti, “Biometric Iris Recognition Based on Hybrid Technique”, International Journal on Soft Computing (IJSC) Vol.2, No.4, November 2011.

[27] Ryan N. Rakvic, Bradley J. Ulis, Randy P. Broussard, Robert W. Ives, Neil Steiner, “Parallelizing Iris Recognition”, IEEE Transactions on Information Forensics and Security, Vol. 4, No. 4, December 2009.

[28] Vanaja Roselin.E.Chirchi, Dr.L.M.Waghmare, E.R.Chirchi, “Iris Biometric Recognition for Person Identification in Security Systems”, International Journal of Computer Applications, Volume 24– No.9, June 2011.

[29] Shreyas Venugopalan, Marios Savvides, “How to Generate Spoofed Irises From an Iris Code Template”, IEEE Transactions on Information Forensics and Security, Vol. 6, No. 2, June 2011.